

## CAPILLARY PHENOMENA, HEAT-AND-MASS EXCHANGE, AND WAVE PROCESSES IN TWO-PHASE FLOW IN POROUS SYSTEMS AND PACKINGS

V. E. Nakoryakov and V. V. Kuznetsov

UDC 532.546+536.25

This article presents the results obtained over the last decade in studies of capillary hydrodynamics, heat-and-mass exchange, and wave processes in two-phase flow in porous beds and packings.

Two-phase and two-fluid flows in porous beds and packings with chaotic and ordered channels of various shapes occur widely in nature and technology. The investigation of this little-studied class of flows is important for developing modern heat-and-mass exchange apparatus and oil and gas production processes, and also for the use of the heat of the Earth's interior. The goal of this work is to obtain the main features of capillary hydrodynamics, heat-and-mass transfer, and wave processes in two-phase and two-fluid flows in porous beds and packings, and also in slotted channels with a slot smaller than the capillary constant over a wide range of flow parameters.

Nakoryakov et al. [1] proposed a physical model for two-phase and two-fluid flows in a porous bed in which capillary forces govern the motion of interfaces both on the scale of an isolated pore and for large ensembles of pores. Below, the flow of two immiscible fluids is treated as a two-phase flow. Previously, the averaged equations of two-phase flow formulated by Masket, Leverett, et al. have been employed in the majority of papers. This approach is based on the use of the empirical functional parameters of two-phase flow, the relative phase permeabilities  $k_i(S_1)$ , where the subscript  $i = 1$  and  $2$  corresponds to the number of phases, and the Leverett functions  $J(S_1)$ , which depend only on the saturation of the pore space of one of the phases. Here the saturation  $S_1$  is the fraction of the pore space occupied by the phase wetting the pore walls. The existing calculation procedures for these relations do not take into account the real geometry of the pores in which the motion of phases occurs. Based on experiments with low-melting Wood alloy, a model for the pore space of typical porous media containing packed quartz sand with grains of the same size and a packing of microspheres was proposed in [1-3]. A single pore is an element of a deformed cubic lattice with pore constrictions having angles  $\varphi$  from  $60$  to  $90^\circ$  (Fig. 1a).

An important feature of two-phase flow is the motion of the interfacial meniscus in pore channels with change in the phase saturation. For the model of a porous bed proposed in [1-3], unified conditions were formulated for the filling of pore constrictions and expansions with phases and for the rupture of the phase that does not wet the pore walls in a pore constriction as a result of the instability of the interface in drain and impregnation. The difference between the phase pressures at which the pore constrictions and expansions are filled with the phase wetting the pore walls varies over wide ranges, and this is responsible for the statistical character of filling of pores with the phases. Figure 1b shows the distribution densities for the drain of a constriction (curve 1), the impregnation of a broadening (curve 2), and the rupture of the nonwetting phase in a constriction (curves 3 and 3') versus the difference in pressure between the phases  $P = p_{1,2}\sigma/R$ . Here  $\sigma$  is the surface-tension coefficient, and  $R$  is the radius of a grain. Curve 3 corresponds to the rupture of the nonwetting phase when the neighboring constrictions are not wetted by the wetting phase, and curve 3' corresponds to the case where they are wetted. The arrows that bound region (A) show the range of pressure difference for drain, when the phases are continuous, and the arrows that bound region (B) show the range of

---

Kutateladze Institute of Thermal Physics, Siberian Division, Russian Academy of Sciences, Novosibirsk 630090. Translated from *Prikladnaya Mekhanika i Tekhnicheskaya Fizika*, Vol. 38, No. 4, pp. 155-166, July-August, 1997. Original article submitted December 17, 1996.

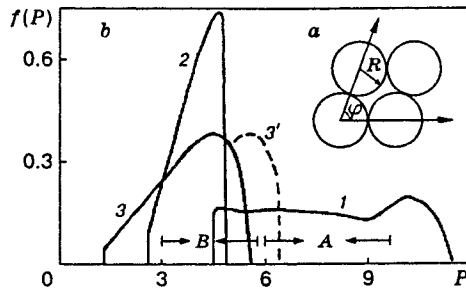


Fig. 1

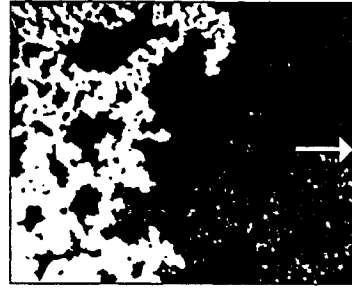


Fig. 2

pressure difference for impregnation. In studies of capillary equilibrium of phases in large ensembles of pores [1–3] methods of percolation theory and numerical calculation have been used. Nakoryakov et al. [1] and Kuznetsov and Dimov [2] solved numerically the problem of filtration in a system of pores and determined the dependence of the saturation of the pore space with a wetting phase on the pressure difference in phases, which gives the Leverett function. The relative phase permeability for a nonwetting phase was calculated within the model of an effectively conducting medium [3]. The exponential law of variation in permeability that follows from percolation theory was taken into account near the filtration threshold.

The previous transparent models of a porous bed do not reflect the main properties of porous channels — volume and random shape. Dimov and Kuznetsov [4] and Vitkovskii et al. [5] developed a two-dimensional transparent model of a porous medium with three-dimensional pores. In this model, the pore space is formed by two glass plates that were tightly pressed to one another by rough surfaces. In the pore space, the dimensions of pore constrictions and expansions vary over wide ranges, and the structural ratio is large.

Figure 2 shows the shape of the interface with displacement of colored water (black liquid) by undecane (white liquid) [2]. The direction of displacement is shown by an arrow. The motion of the displacement front proceeds as rare random jumps of the meniscus with leakage in neighboring pores. The microstructure of the displacement front has been studied for drain and impregnation with initial saturation of the capillary-entrapped phase and without it [2, 3, 6]. With increase in the capillary number  $Nc = v\mu/\sigma$  ( $\mu$  is the viscosity,  $\sigma$  is the interfacial tension, and  $v$  is the reduced velocity), the fractal dimension of the interface remains unchanged and is equal to 1.34, and the self-similarity scale decreases, reaching the pore size [6]. The pore space is a fractal, and the retention of the fractal dimension of the interface shows that capillary forces completely determine the motion of menisci inside the self-similarity region. If the dimension of this region far exceeds the pore size, percolation-like clusters of two phases develop at the displacement front, and the functional parameters corresponding to steady flow can be used.

To verify this statement experimentally, Vakhitov et al. [7] studied the structure of two-phase flow with immiscible displacement in packed quartz sand filling a tube located horizontally. Water saturation was measured by resistive gauges. For the displacement of hydrocarbon fluids of various density by water, experimental data agree well with calculations by the averaged equations. In the one-dimensional case for the normalized saturation of the phase displacer  $S$ , these equations reduce to the Rapoport–Lis equation

$$\frac{\partial S}{\partial t} + F'(S) \frac{\partial S}{\partial x} - \varepsilon \frac{\partial}{\partial x} \left( a(S) \frac{\partial S}{\partial x} \right) = 0. \quad (1)$$

Here the functions  $F(S)$  and  $a(S)$  are determined by the functions  $k_i(S)$  and  $J(S)$  and by the ratio of the viscosities of the phases [8],  $\varepsilon = \sigma\sqrt{km}/(\mu_2 v_0 L)$  (where  $k$  is the permeability,  $m$  is the porosity,  $v_0$  is the reduced velocity at the inlet,  $\mu$  is the viscosity of the displaced liquid, and  $L$  is the length of the region occupied by the porous medium), the longitudinal coordinate and time are made dimensionless with respect to  $L$ ,  $v_0$ , and  $m$ , the functional parameters are determined for steady flow, and the prime denotes differentiation with respect to  $S$ .

The greatest difficulties in the experimental measurement of  $k_i(S)$  and  $J(S)$  arise because of their behavior near the threshold of filtration of the phases. Bocharov et al. [8] studied numerically the effect of

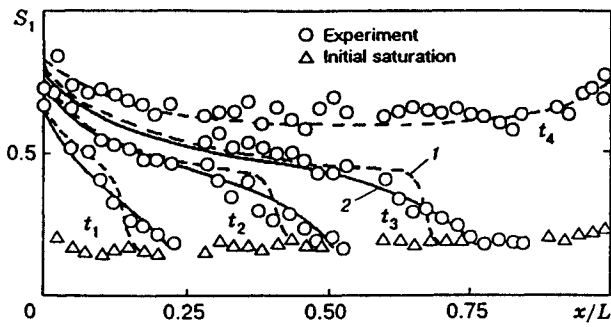


Fig. 3

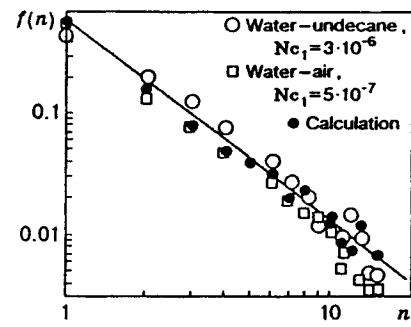


Fig. 4

the behavior of the functional parameters on the flow with immiscible displacement. It has been shown that the behavior of  $k_i(S)$  near the thresholds of filtration of the phases affects significantly the structure of the displacement front, and the occurrence of two- and multiwave fronts is possible.

The stepped equilibrium filling of the pore channels cannot be sustained by capillary forces at a high rate of variation in the phase saturation [9]. The increase in the pressure difference between the phases disturbs the order of filling of the pore channels, and the functional parameters  $k_i$  and  $J$  are determined by the effective rather than by the true saturation. The effective saturation is determined from the formula

$$\alpha(S) = S + DR(S) \frac{\partial S}{\partial t}.$$

The equilibrium parameter  $D$  and the function of nonequilibrium  $R(S)$  are determined [9] based on the mechanism of formation of conducting clusters of phases. Substituting  $\alpha(S)$  for the true saturation in the functional dependences  $F(S)$  and  $\alpha(S)$  in Eq. (1) [9] leads to a system of equations of nonequilibrium filtration. A similar model of nonequilibrium filtration was earlier proposed by G. I. Barenblatt, but without the calculation procedure for the nonequilibrium parameter. The equations of nonequilibrium filtration were solved numerically [9–12] for various values of  $\epsilon$ ,  $D$ , and the functional parameters for displacement in strictly hydrophilic porous media and with nearly neutral wetting. In this case, the nonequilibrium effects manifest themselves for lower value of the capillary number  $Nc_2$  (the subscript 2 corresponds to the displaced phase) because of the smallness of  $J(S)$  over a wide range of saturation values. A comparison of the calculated saturation profiles of the liquid displacer with the experimental data for four times ( $t_1 = 0.28$ ,  $t_2 = 0.7$ ,  $t_3 = 1.22$ , and  $t_4 = 4.9$ ) and for a strictly hydrophilic porous media ( $Nc_2 = 4.7 \cdot 10^{-5}$  and  $\mu_2/\mu_1 = 17$ ) is shown in Fig. 3 [9, 12]. Curve 1 corresponds to the calculation by the equilibrium model, and curve 2 corresponds to the calculation by the nonequilibrium model. The experiments were performed in a thin layer of quartz sand. The distribution of the saturation  $S_1$  over the length was obtained by the radioisotope method. Nonequilibrium is pronounced near the front, and this rules out high saturation gradients. When the wetting is nearly neutral, the function of nonequilibrium  $R(S)$  takes large values over a wide range of saturations of the phases. In this case, for large values of the nonequilibrium parameters, a sudden decrease in the saturation at the displacement front is observed both in the experiments and in calculations [9, 12].

With decrease in the phase saturation, capillary entrapment of the phases occurs. This process was investigated in a number of papers, but the effect of the real geometry and chaotic microstructure of pores on the formation of a capillary-entrapped phase and conditions of its extraction still remain to be studied. Kuznetsov and Dimov [2, 3, 6] studied numerically the displacement of both a wetting phase and a nonwetting phase from a porous bed with allowance for the micromechanics of motion of menisci and entrapment of phases. The calculations were performed on a grid model of a porous medium with a net of channels that were randomly distributed in size and connected nodes of various diameters. The filling of nodes and connections with the phases was performed using conditions of drain and impregnation and rupture of the nonwetting phase in constrictions within the framework of the transparent model of a porous medium. After displacement, the integrity of the conducting cluster is disturbed, and it breaks up into capillary-entrapped clusters of different

sizes. Kuznetsov and Dimov [3, 6] obtained the size distribution of ganglia clusters. Figure 4 shows the exponential dependence of the number of clusters on their sizes for the displacement of undecane and air by water. The capillary number  $N_{c1}$  corresponds to the continuous phase. The curve is the standard deviation from the calculation results. The calculation results agree well with the experimental data obtained using the transparent model for flows with various capillary numbers.

Conditions under which ganglia of various sizes can move downstream have been studied experimentally [4]. Capillary numbers for which a ganglion begins to move were determined. For a porous medium with a large structural ratio, it is most probable that a ganglion breaks up during its motion. The motion of ganglia of arbitrary shape and size in the grid model of a porous medium was studied with allowance for the possibility that the liquid wetting the porous medium can leak into a pore constriction. For the given distributions of structural parameters of a porous medium, a statistical analysis of the stepped motion of an ensemble of noninteracting ganglia was performed [3, 4]. The probability of a ganglion leaking into a neighboring pore with variation in the value of  $N_{c1}$  and the number of pores occupied by the ganglion were established. In addition, the probabilities of a ganglion leaking into a neighboring pore with rupture in even one pore constriction, without rupture, and with preservation of the ganglion position were determined. In a porous medium with a large structural ratio, the probability that an isolated ganglion moves over the lattice sites will be high only for a ganglion having a smaller volume than the pore volume. If the volume of a ganglion is larger than the pore volume, continuous fragmentation of the ganglion occurs without significant change in saturation of the nonwetting phase. This explains the threshold character of variation in the saturation of natural cores with oil with increase in the capillary number.

Kuznetsov and Dimov [2, 3, 6] studied experimentally the behavior of a large accumulation of ganglia with jumpwise increase in  $N_{c1}$ . If the density of ganglia is high, they interact during motion, and large unsteady clusters arise which move downstream. However, for  $N_{c1} < 10^{-3}$ , fragmentation of ganglia is the most probable, and outflow of the nonwetting phase from the pore medium is small. The same authors obtained a stationary size distribution of capillary-entrapped clusters for various values of  $N_{c1}$ . With increase in  $N_{c1}$ , the fraction of clusters with volumes smaller than the pore volume increases, in complete agreement with the results of statistical analysis. Using the probability of steady positions of ganglia of various sizes as the weight function for the initial distribution, Kuznetsov and Dimov [6] obtained the size distribution of ganglia for various values of  $N_{c1}$ , which agrees well with the experimental data.

The stability of the front and the development of fingers in homogeneous and layered inhomogeneous porous media with immiscible displacement in which the more viscous liquid displaces the less viscous liquid were studied in [5, 13–19]. “Viscous fingering” has been studied previously on the simplest model of a porous medium, a narrow slot between parallel plates (the Hill–Shaw) cell. This model does not take into account the random arrangement of pores and is too simplified to describe two-phase flow. Vitovskii et al. [5], Bocharov et al. [16], and Kuznetsov et al. [18, 20] performed experiments on a horizontally located, transparent model of a porous medium formed by rough glasses which were tightly pressed to one another, and in a layer of quartz sand. The porous medium was saturated by hydrocarbon liquids with elevated viscosity or a water–glycerin solution, which were displaced by colored water or kerosene. To measure the saturation field, a mercury radioisotope was introduced into the water phase. The spatial distribution of gamma radiation was recorded by a gamma chamber with a high-resolution collimator.

The displacement front is formed by capillary menisci that separate the liquids. The motion of the menisci is random. This leads to the occurrence of flow in which capillary forces govern the propagation of the front on a small scale and generate noise, and viscous forces are responsible for the global flow instability on a large scale [5, 20]. A typical shape of fingers for unstable displacement was obtained in [5, 20] and is shown in Fig. 5, where  $M_c$  is the ratio of phase mobilities at the displacement front. The flow direction is shown by an arrow. This is a cellular structure of the front with stable cells (Fig. 5a) and fingers growing with time (Fig. 5b and c). The displacement is significantly nonequilibrium, and the self-similarity region is of the order of the pore size. The growth of the fingers is accompanied by branching [5, 20]. In the initial stage of development of the fingers, branching is absent, suppression of slowly growing fingers occurs, and the width of rapidly growing fingers increases. The capillary instability on a small scale generates disturbances of the

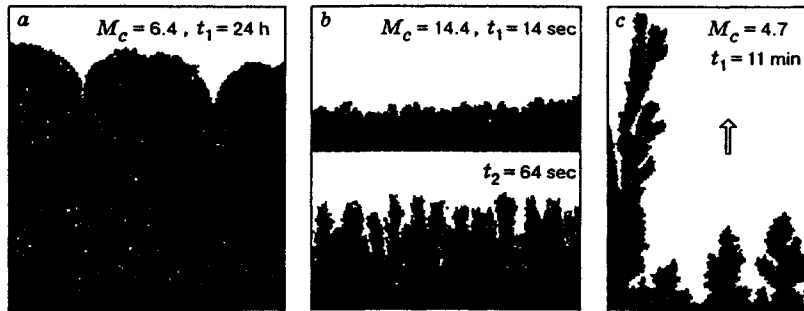


Fig. 5

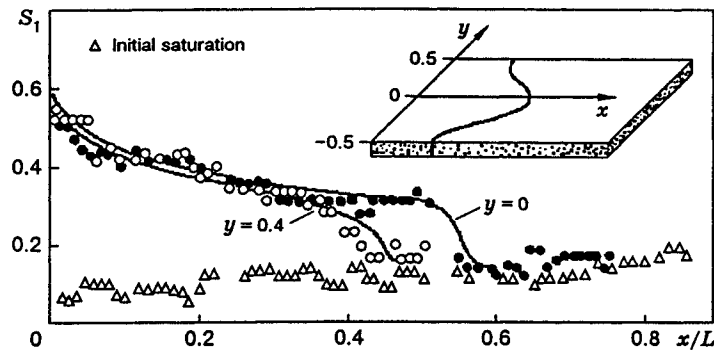


Fig. 6

velocity field, and supercritical bifurcations cause branching of fingers when the width of the fingers is larger than the threshold value  $\lambda_{cr}$ . Vitovskii et al. [5] obtained good agreement between the experimental values of  $\lambda_{cr}$  and calculations using the theory of supercritical bifurcations. The active branching of fingers decreases their mutual influence, and the displacement regime is given by the relation between the transverse dimension of the displacement region  $H$  and the value of  $\lambda_{cr}$ . A chart of typical displacement regimes of fingers for given levels of random disturbances, which determine  $\lambda_{cr}$ , is constructed in [5, 20].

When the displacement is equilibrium over the entire flow region, the saturation values of the phases are variable, and the viscosity instability of the displacement front deforms the field of isosats (isolines of constant saturation  $S_1$ ). The structure and dynamics of fingers in a sand layer have been studied experimentally [16, 18, 20]. The growth rate and limiting length of fingers were determined. The development of fingers has been simulated numerically [13–15, 18–20] using dimensionless equations of two-phase filtration written in the variables  $S$  (normalized saturation) and  $p$  (effective pressure):

$$\frac{\partial S}{\partial t} = \text{div}(\epsilon a(S) \text{grad } S - v F(S)), \quad \text{div}(v) = 0, \quad v = -M(S) \text{grad } p. \quad (2)$$

Here the functions  $a(S)$ ,  $F(S)$ , and  $M(S)$  are determined by the viscosities of the liquids and by the functional parameters  $k_i(S)$  and  $J(S)$ ; the equations are made dimensionless with respect to the width of the cell in which the finger grows and the reduced velocity at the entrance.

Data on the structure of growing fingers have been obtained under various conditions. The distributions of the saturation  $S$  in a sand layer of length  $L$  for the head ( $y = 0$ ) and tail ( $y = 0.4$ ) parts of the fingers for  $\mu_2/\mu_1 = 17$  and  $t = 0.5$  are shown in Fig. 6. The numerical-calculation results (curves) and the experimental data (points) for both the finger structure and growth rate are in good agreement. With increase in the finger length, the capillary flow from the head part to the tail part of the finger increases. The growth rate of the finger then decreases, and a limiting length can be established. Bocharov and Kuznetsov [15] obtained an

approximate relation for the limiting length of fingers.

A theoretical analysis of the displacement in a layered inhomogeneous porous medium and numerical calculations using Eqs. (2) for a two-layer porous medium were performed in [17]. In a two-layer porous medium, fingers grow in the layer with a higher permeability. An approximate relation for the limiting length of a finger in a two-layer porous medium with displacement stabilized by capillary flows was obtained. The limiting length of the finger  $l_f$  is defined by the dimensionless parameter

$$\varepsilon_H \sqrt{k_2/k_1} = \sigma \sqrt{k_2 m} / (v_0 \mu_2 H),$$

where  $k_2$  is the permeability of the low-permeable layer, and  $H$  is the total thickness of the layers, which also depends on the relation between the thicknesses of the layers and the viscosities of the liquids. Kuznetsov et al. [17] studied experimentally the displacement in a two-layer medium. Good agreement between experimental data and numerical results is obtained.

For one-phase flow in a porous medium, deviation from the Darcy law takes place even for  $Re_d > 10$ . Evseev et al. [21, 22] studied the hydrodynamics of turbulent flow in a packing of glass spheres using a laser Doppler anemometer. Optical deviations due to the reflection of the beam from the curvilinear surfaces of spheres were eliminated by using a liquid having the same refraction index as glass. Evseev et al. [21] studied the hydrodynamics of flow in a cubic packing of spheres. Flow visualization using a laser knife was performed. A system of vortices in the schlieren region behind the spheres was detected, and spectral characteristics of the pulsations of the longitudinal velocity with a continuous spectrum was obtained. The flow through channels in the cubic packing corresponds to a turbulent jet with a turbulence factor of the order of 5–10%. Return flow due to flow separation was observed in the schlieren region behind the points of contact of spheres. In the mixing zone, the turbulence factor reached 22–24%.

The octahedral packing of spheres differs from the cubic packing in that the channels between the spheres are not through but are curved. Flow visualization showed that, in this case, the jet that arises in the narrow section between the spheres is divided downstream into four jets, and they then merge again into one jet. The longitudinal velocity profiles in the minimum section of the octahedral packing have two maxima located near the points of contact of the spheres. The transverse-velocity components are different from zero only near the points of contact. The pulsations of all three velocity components are approximately equal, and their level is 2–2.5 times higher than that for the cubic packing. The flow-separation zones located behind the points of contact of spheres have a strong effect on the turbulent-flow structure at high Reynolds numbers.

Heat-and-mass exchange in two-phase flow in a tube and in an annulus with a packing of spheres was studied in [23–27]. The longitudinal unsteady mass transfer of a completely soluble admixture for one-phase flow and for flow with incomplete saturation in a packing of spheres and in the two-dimensional transparent model of a porous medium was studied in [24]. Theoretical analysis of mass transfer takes into account the geometry of the pore space and the percolation nature of the two-phase flow. The longitudinal dispersion  $D_L$  for one-phase flow is mainly determined by the time of transfer of labeled particles by molecular diffusion along the pore walls. The capillary-entrapped gas phase introduces a new typical dimension, the cluster size. Clusters have a very developed shape and can occupy many pores, but their transverse size does not exceed the pore size, as a rule. Taking this into account, Kuznetsov [24] obtained an expression for the longitudinal dispersion coefficient for flow with incomplete saturation. Figure 7 shows the longitudinal dispersion coefficient measured in a tube with a packing of spheres and divided by the diffusion coefficient in the liquid (points 1 refer to flow with complete saturation, points 2 refer to  $S_2 = 0.22$ , and points 3 to  $S_2 = 0.25$ ), and the calculation data (curve 1 refers to one-phase flow and curves 2 refers to flow with incomplete saturation). The saturation  $S_2$  corresponds to the fraction of the pore volume occupied by the gas. The experiments were performed in a tube filled with glass spheres 1.2 mm in diameter for flow of a salt solution with a time-dependent concentration. The previous experimental data on mass transfer for one-phase flow are located between curves 3. For flow with incomplete saturation, the longitudinal dispersion coefficients increase considerably (by a factor of up to three) compared with one-phase flow. An even larger (by an order of magnitude) increase is observed for flow in the transparent model of a porous medium.

The heat exchange with the wall for upward gas-liquid flow in a tube filled with spheres was studied in

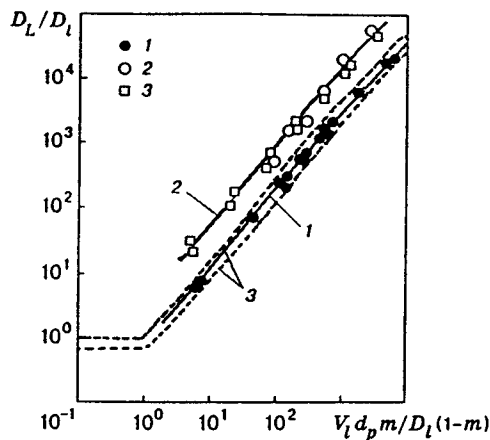


Fig. 7

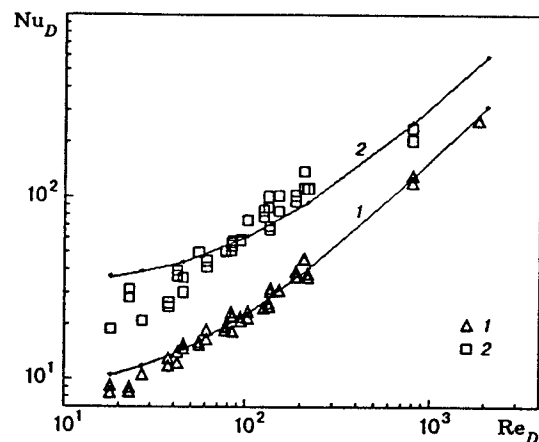


Fig. 8

[23, 24]. For one-phase flow, Kuznetsov et al. proposed a two-layer model of heat exchange with the wall taking into account the elevated porosity and decreased radial heat conductivity in the wall layer. The experiments were performed in a heated tube filled with glass spheres. Figure 8 shows the coefficient of heat removal from the wall normalized over the tube diameter  $D$  versus the Reynolds number  $Re_D$ . Points 1 correspond to the experimental data for one-phase flow, and points 2 correspond to the maximum intensity of heat exchange for two-phase flow. For one-phase flow, the experimental data correspond to the proposed two-layer heat exchange model (curve 1) over a wide range of Peclet ( $Pe$ ) numbers. In the region of unsteady bubble and slug two-phase flows, the volumetric longitudinal heat transfer is considerably enhanced, and the heat-removal coefficient increases. This effect practically disappears in going over to the capillary flow regime. Curve 2 shows the calculated heat-exchange coefficient in the region of greatest intensity of heat exchange.

The heat exchange in flow past a cylindrical heat-releasing element in a packing of spheres was studied experimentally in [25–27]. A stainless tube with thermocouples located on the wall was used as the vertical heat-releasing element. Freon R318C was the heat carrier in the regime of one-phase convection and underheated boiling. The heat-exchange coefficient and the critical heat flux were measured over a wide range of heat fluxes and velocities of the heat carrier. In the region of one-phase flow, the heat-exchange coefficient corresponds to the calculation by the two-layer model of heat exchange. In boiling, the heat-exchange coefficient follows the boiling curve for a large volume over a wide range of flow velocities. The high pressure gradients in the working section lead to small separation diameters of vapor bubbles, and the experimental data on the critical heat flux correspond to the Kutateladze–Leont’ev dependence for high-velocity flows in tubes.

Nakoryakov et al. [28, 29] studied sheet boiling on a plate embedded in a granular medium using the following assumptions: the flow of the phases proceeds at low velocities and the Darcy approximation is valid, the vapor temperature is equal to the saturation temperature, the friction at the condensate–vapor interface is equal to zero, and the physical properties of the liquid do not depend on the temperature. The analytical solution of [28] was obtained under the assumption that the heat in the liquid is transferred only by the effective longitudinal heat conductivity. This solution agrees well with the experimental heat-removal coefficients obtained in [29].

Mukhin et al. [30] and Nakoryakov and Petrik [31] present the results of theoretical and experimental studies of sheet condensation on an inclined surface in a porous medium. The velocity profile in the condensate sheet is determined using the Darcy approximation, and the Brinkman approximation is used near the wall. In the analytical solution, it was assumed that the heat in the sheet was transferred only by the effective longitudinal heat conductivity. The solution obtained was compared with the experimental heat-exchange coefficients for the condensation of R12 Freon vapor in quartz sand and in packings of Nichrome and glass microspheres. The relation  $Nu = 2ArPrK$  was obtained under the assumption of constant effective heat

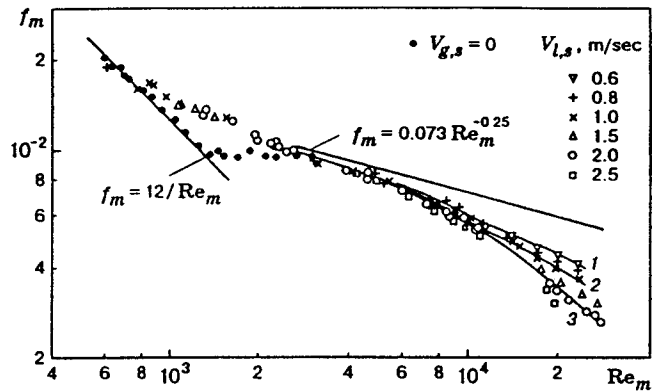


Fig. 9

conductivity. Here the Archimedeian number is derived from the permeability of the porous medium and the length of the working section,  $Pr$  is the Prandtl number, and  $K$  is the Kutateladze number. The numerical results agree well with the experimental data with variation of the  $Ar Pr K$  complex from 200 to  $4 \cdot 10^4$ .

Kuznetsov and Vitovskii [32] and Nakoryakov et al. [33] studied upward gas-liquid flow in a slotted channel as an element of fractured porous media. Upward air-water flow was studied in a Plexiglas annulus with a narrow slot. Flow visualization was performed over a wide range of reduced liquid and gas velocities. When the slot dimension is smaller than the capillary constant, interfaces are formed by the menisci between the channel walls. This leads to the following characteristic types of two-phase flow: turbulent flow with small noninteracting bubbles, layered flow, flow with large Taylor bubbles, and two-phase cellular flow with constrictions of liquid plugs. The last two types of flow are essentially unsteady with large pressure pulsations. Based on the data for the flow structure, a model of two-phase flow in a slotted channel was constructed, and friction losses were determined. Figure 9 shows the friction coefficient versus the Reynolds number of the mixture. The points show the experimental data and curves 1-3 are the calculation results for the reduced liquid velocities  $V_{l,s} = 0.6, 1.0, \text{ and } 2.0$  m/sec, respectively. With increase in  $V_{l,s}$ , the deviation of the experimental data from the calculated data for homogeneous flow increases.

Wave processes in saturated porous media were studied in [34-36]. The propagation of pressure waves in loose and packed porous media saturated with a liquid were examined in [34, 35]. In packed layers and porous media saturated with a gas-liquid medium, the nonequilibrium due to inertial effects upon pressure equalization in the phases should be taken into account along with the nonequilibrium due to equalization of temperature and phase velocities. For a porous medium saturated with a liquid with gas bubbles, Nakoryakov et al. [36] obtained the Rayleigh equation, which relates the pressures in the liquid and gas phases during bubble oscillations. Using the Rayleigh equation as the closing relation, the same authors [36] obtained a system of equations describing the propagation of finite-amplitude pressure waves in a porous medium saturated with gas bubbles. For small times, the solution gives two longitudinal waves in a porous medium: a "fast" wave and a "slow" wave, which can propagate independently. For the "fast" wave, the decay is small and the dispersion effects due to bubble oscillations are significant. The propagation velocity of the "fast" wave is mainly determined by the compressibility of the solid frame, and the structure is determined by the bubble dynamics in the wave. A porous medium saturated with a liquid and bubbles is characterized by the bulk elastic moduli of the solid frame and of the gas-liquid mixture. In the "fast" wave, the solid frame and the liquid are deformed in phase, and the wave attenuation is very insignificant. In the "slow" wave, the deformations proceed in antiphase, and the wave attenuation due to interfacial friction increases suddenly with increase in gas content.

The propagation of pressure waves in a saturated porous medium and a liquid with gas bubbles was studied experimentally in a vertical "shock" tube in [34-36]. The working section was filled with packed quartz sand or a sintered packing of organic-glass spheres of small size, which were saturated with liquids with various



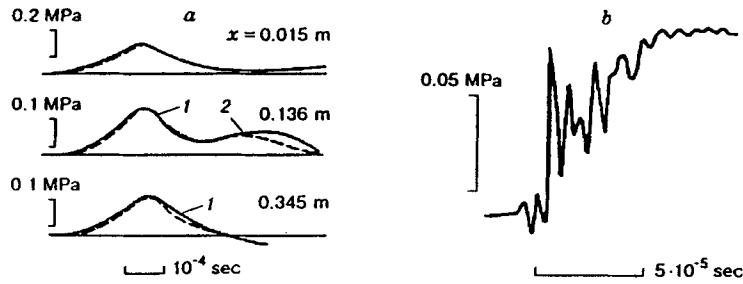


Fig. 10

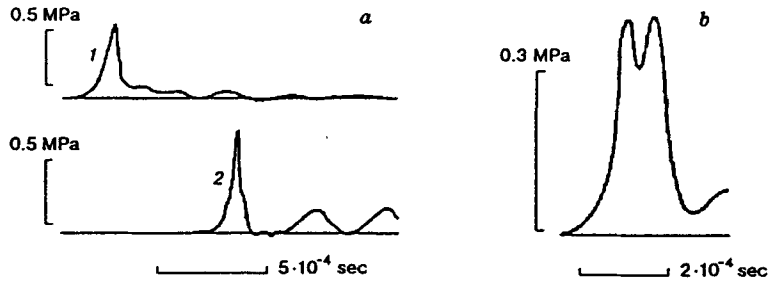


Fig. 11

viscosities and capillary-entrapped gas bubbles. With the propagation of pressure waves in a consolidated porous medium saturated with a liquid or a gas-liquid mixture, two types of waves were observed at small distances from the entry: a "fast" wave (1) and a "slow" wave (2) (Fig. 10a). The experimental pressure profile at distance  $x$  from the place where a wave enters a sintered packing of spheres completely saturated with benzene is shown in Fig. 10a by the solid curve. Figure 10b shows the wave profile for incomplete saturation ( $S_2 = 0.0036$ ). At large amplitudes, the "fast" wave has an oscillating structure, which is due to the bubble dynamics, and a typical relaxation elevation behind the wave front. The measured wave velocities and attenuation intensities are in good agreement with the calculations (the dashed curve in Fig. 10a) for both the porous medium completely saturated with liquids [35] and for the liquid with capillary-entrapped bubbles [36]. The formation of the "fast" and "slow" waves at the entry to the medium was investigated in [34-36]. With the propagation of pressure waves in packed sand, only one longitudinal wave was observed [35]. In this case, the main mechanism of wave attenuation is dry friction at grain contacts during grain repacking in the wave.

The dispersion effects due to the inertia of the attached mass of gas inclusions are most pronounced in a liquid with gas bubbles and without a porous bed. For this medium, solitons, wave trains, and oscillating shock waves have been previously detected and investigated, and their interaction has been studied. Nakoryakov et al. [37] showed that, at large amplitudes, solitons have a sharpened shape (Fig. 11a). Pressure profiles were obtained in a water-glycerin solution with  $\text{CO}_2$  bubbles (bubble radius 1.2 mm) at  $x = 0.07$  (curve 1) and 0.165 m (curve 2). The bubbles in a pressure wave can be considered as nonlinear oscillators, and their interaction for bubbles of two different sizes leads to the occurrence of multisolitons or oscillating solutions [38]. A typical multisoliton in a water-glycerin solution with  $\text{CO}_2$  bubbles (the bubble radii are 0.6 and 1.2 mm, and the ratio of their volume gas contents is 0.3) is shown in Fig. 11b. Dontsov et al. [39] constructed a chart of typical structures of multisolitons versus the wave amplitudes and the fraction of large bubbles in the total gas content. The experiment of Nakoryakov et al. [37] with gases having different thermophysical properties showed that wave attenuation over a wide range of amplitudes is caused mainly by the heat exchange between the gas in bubbles and the liquid during bubble collapse in the waves.

## REFERENCES

1. V. E. Nakoryakov, V. V. Kuznetsov, and V. V. Dimov, "A physical model of two-phase flow in a porous media," in: *Exploitation of Condensed-Gas Deposits: Proc. Int. Conf.*, Krasnodar (1990).
2. V. V. Kuznetsov and S. V. Dimov, "The microstructure of two-phase flow in a porous medium," in: *Hydrodynamics and Heat-and-Mass Transfer in Porous Media* (Collected scientific papers) [in Russian], Inst. of Thermal Physics, Novosibirsk (1991), pp. 71–88.
3. V. V. Kuznetsov and S. V. Dimov, "The influence of the geometrical parameters of a porous medium on two-phase filtration," in: *4th Symp. Multiphase Transport in Porous Media: Proc. ASME Winter Annual Meeting*, New Orleans, Nov. 27–30 (1993), pp. 207–223.
4. S. V. Dimov and V. V. Kuznetsov, "Conditions of mobilization of a nonwetting phase in a porous medium," *Izv. Akad. Nauk, Mekh. Zhidk. Gaza*, No. 6, 104–111 (1988).
5. O. V. Vitovskii, V. V. Kuznetsov, and V. E. Nakoryakov, "The stability of the displacement front and 'fingering' in a porous medium," *Izv. Akad. Nauk, Mekh. Zhidk. Gaza*, No. 5, 101–106 (1989).
6. V. V. Kuznetsov and S. V. Dimov, "The micromechanics of formation of residual saturation with immiscible displacement in a porous medium," *Izv. Akad. Nauk, Mekh. Zhidk. Gaza*, No. 3, 116–121 (1994).
7. V. G. Vakhitov, S. V. Dimov, O. V. Vitovskii, and V. V. Kuznetsov, "An experimental study of the displacement of hydrocarbons by water in porous media," Abstracts of the VIth All-Union Conf. on Theoretical and Applied Mechanics, Tashkent, 95–96 (1986).
8. O. B. Bocharov, V. V. Kuznetsov, and Yu. V. Chekhovich, "On the structure of solutions of the Rapoport–Lis problem," in: *Dynamics of Continuous Media* [in Russian], Novosibirsk, 85 (1988), pp. 13–21.
9. O. B. Bocharov, O. V. Vitovskii, and V. V. Kuznetsov, "The structure of saturation jumps with nonequilibrium displacement in porous media," *Izv. Akad. Nauk, Mekh. Zhidk. Gaza*, No. 6, 97–104 (1990).
10. O. B. Bocharov, V. V. Kuznetsov, and Yu. V. Chekhovich, "On the nonequilibrium two-phase filtration in a porous medium," in: *Simulation in Mechanics* [in Russian], Inst. of Theor. and Appl. Mech., Sib. Div., Acad. of Sci. of the USSR, 3, No. 2, (1989), pp. 47–53.
11. O. B. Bocharov, V. V. Kuznetsov, and Yu. V. Chekhovich, "Numerical study of the nonequilibrium filtration of immiscible liquids," *Inzh.-Fiz. Zh.*, 57, No. 1, 91–95 (1989).
12. O. B. Bocharov, O. V. Vitovskii, V. V. Kuznetsov, and Yu. V. Chekhovich, "Nonequilibrium displacement in a porous medium," in: *Numerical Methods of Solution of Filtration Problems* (Collected scientific papers) [in Russian], Inst. of Theor. and Appl. Mech., Novosibirsk (1989), pp. 34–39.
13. O. B. Bocharov and V. V. Kuznetsov, "Numerical simulation of unsteady displacement in a porous medium," in: *Numerical Methods of Solution of Filtration Problems for a Multiphase Incompressible Liquid* (Collected scientific papers) [in Russian], Inst. of Theor. and Appl. Mech., Novosibirsk, 48–54 (1987).
14. O. V. Bocharov and V. V. Kuznetsov, "Development of viscosity instability in a porous medium," *Prikl. Mekh. Tekh. Fiz.*, 30, No. 2, 116–120 (1989).
15. O. V. Bocharov and V. V. Kuznetsov, "Development of viscosity instability in a porous medium with allowance for capillary forces," *Izv. Akad. Nauk, Mekh. Zhidk. Gaza*, No. 1, 115–120 (1980).
16. O. V. Bocharov, O. V. Vitovskii, Yu. P. Kolmogorov, and V. V. Kuznetsov, "Experimental study of viscous instability in a porous medium," *Prikl. Mekh. Tekh. Fiz.*, 30, No. 4, 79–84 (1989).
17. V. V. Kuznetsov, V. E. Nakoryakov, and S. A. Safonov, "Fingering in immiscible displacement in a two-layer porous medium," *Izv. Akad. Nauk, Mekh. Zhidk. Gaza*, No. 6, 98–104 (1990).
18. V. V. Kuznetsov, O. V. Bocharov, and O. V. Vitovskii, "Viscous fingering in a porous medium," in: *Hydrodynamics and Heat-and-Mass Exchange in Porous Media* (Collected scientific papers) [in Russian], Inst. of Thermal Physics, Novosibirsk (1991), pp. 41–70.

19. O. V. Bocharov and V. V. Kuznetsov, "Effect of capillary forces on the viscous instability regime in a porous medium," *Sib. Fiz. Tekh. Zh.*, No. 3, 54–58 (1991).
20. V. V. Kuznetsov, O. V. Bocharov, and O. V. Vitovsky, "Viscous fingering and surface structure formation in porous media," in: *Instabilities in Multiphase Flows: Proc. Int. Symp. on Instabilities in Multiphase Flows* (Rouen, France, May 11–14, 1992), Plenum Press, New York (1993), pp. 309–320.
21. A. R. Evseev, V. E. Nakoryakov, and N. N. Romanov, "Local structure of the filtration flow in a cubic packing at large Reynolds numbers," *Izv. Akad. Nauk. SSSR, Ser. Tekh. Nauk*, No. 1, 51–56 (1989).
22. V. E. Nakoryakov, A. R. Evseev, and N. N. Romanov, "Experimental investigation of the turbulent filtration flow," *Int. J. Multiphase Flow*, 17, No. 1, 103–118 (1991).
23. V. V. Kuznetsov, S. B. Chikov, and S. Yu. Saltanov, "Heat transfer in a packed bed with gas (vapor)–liquid cocurrent flow," *Russ. J. Eng. Thermophysics*, 5, 205–221 (1995).
24. V. V. Kuznetsov, "Heat and mass transfer in a packed bed with cocurrent two-phase flow," in: *Porous Media and Their Applications in Science, Engineering and Industry: Proc. Int. Conf.*, Kona, U.S., June 16–21 (1996), pp. 241–264.
25. V. V. Kuznetsov, Yu. S. Borchevkin, and S. B. Chikov, "Forced convection cooling of a surface embedded in porous structure," in: *Evaporative Cooling Systems of Electronic Equipment: Proc. Int. Seminar*, Novosibirsk (1993). pp. 177–186.
26. V. V. Kuznetsov and S. B. Chikov, "Forced convection cooling of a surface embedded in a porous structure," in: *Heat Transfer: Proc. 1st Europ. Conf. on Thermal Sciences*, Birmingham, UK, Sept. 16–18, 1992. Hemisphere Pub. Corp. (1992), Vol. 2, pp. 1099–1105.
27. V. V. Kuznetsov and S. B. Chikov, "Heat exchange in the longitudinal flow of a heat-releasing element in a porous medium," *Teplofiz. Vys. Temp.*, 31, No. 2, 281–285 (1993).
28. V. E. Nakoryakov, V. A. Mukhin, P. T. Petrik, and I. V. Dvorovenko, "Sheet boiling in a granular medium," in: *Hydrodynamics and Heat-and-Mass Exchange in Porous Media* (Collected scientific papers) [in Russian], Inst. of Thermal Physics, Novosibirsk, (1991) pp. 31–40.
29. V. E. Nakoryakov, V. A. Mukhin, P. T. Petrik, and I. V. Dvorovenko, "Sheet boiling in a granular medium," *Russ. J. Eng. Thermophysics*, 2, No. 4, (1992), pp. 205–221.
30. V. A. Mukhin, V. E. Nakoryakov, P. T. Petrik, and G. S. Serdakov, "Vapor condensation on an inclined plate within a porous medium," *Prikl. Mekh. Tekh. Fiz.*, 26, No. 5, 85–90 (1985).
31. V. E. Nakoryakov and P. T. Petrik, "Condensation in granular media," *Russ. J. Eng. Thermophysics*, 2, No 4 (1994), pp. 299–310.
32. V. V. Kuznetsov and O. V. Vitovskii, "Experimental investigation of upward gas–liquid flow in vertical narrow annuli," in: *Experimental Heat Transfer, Fluid Mechanics, and Thermodynamics: Proc. 2th World Conf.* (Dubrovnik, Yugoslavia, June 23–28, 1991), Elsevier, New York (1991), pp. 1120–1126.
33. V. E. Nakoryakov, V. V. Kuznetsov, and O. V. Vitovskii, "Experimental investigation of upward gas–liquid flow in a vertical narrow annulus," *Int. J. Multiphase Flow* 18, No 3, 313–326 (1992).
34. V. E. Nakoryakov, V. V. Kuznetsov, and V. E. Dontsov, "Pressure waves in porous media," in: *Problems of Nonlinear Acoustics: Proc. of IUPAP — IUTAM Symp. on Nonlinear Acoustics*, Novosibirsk (1987), pp. 108–112.
35. V. E. Dontsov, V. V. Kuznetsov, and V. E. Nakoryakov, "Propagation of compression waves in a porous fluid-saturated medium," *Prikl. Mekh. Tekh. Fiz.*, 29, No. 1, 120–130 (1988).
36. V. E. Nakoryakov, V. V. Kuznetsov, and V. E. Dontsov, "Pressure waves in saturated porous media," *Int. J. Multiphase Flow*, 15, No 6, 857–875 (1989).
37. V. E. Nakoryakov, V. V. Kuznetsov, V. E. Dontsov, and P. G. Markov, "Pressure waves of moderate intensity in liquid with gas bubbles," *Int. J. Multiphase Flow* 16, No. 5, 741–749 (1990).
38. V. G. Gasenko, V. E. Dontsov, V. V. Kuznetsov, and V. E. Nakoryakov, "Oscillating solitary waves in a liquid with gas bubbles," *Izv. Sib. Otd. Akad. Nauk SSSR, Ser. Tekh. Nauk*, 21, No. 6, 43–45 (1987).
39. V. E. Dontsov, V. V. Kuznetsov, P. G. Markov, and V. E. Nakoryakov, "Propagation of pressure waves in a liquid with gas bubbles of various sizes," *Akust. Zh.*, 34, No. 1, 157–159 (1989).